

Follow-the-Leader Deployment of Steerable Needles Using a Magnetic Resonance-Compatible Robot With Stepper Actuators¹

E. Bryn Pitt

Department of Mechanical Engineering,
Vanderbilt University,
Nashville, TN 37235

David B. Comber

Department of Mechanical Engineering,
Vanderbilt University,
Nashville, TN 37235

Yue Chen

Department of Mechanical Engineering,
Vanderbilt University,
Nashville, TN 37235

Joseph S. Neimat

Department of Neurological Surgery,
Vanderbilt University Medical Center,
Nashville, TN 37232

Robert J. Webster, III

Department of Mechanical Engineering,
Vanderbilt University,
Nashville, TN 37235

Eric J. Barth

Department of Mechanical Engineering,
Vanderbilt University,
Nashville, TN 37235

1 Background

Epilepsy is a debilitating, potentially fatal, seizure-causing neurological disorder that will affect approximately 1% of people worldwide in their lifetimes [1]. Medication-based treatment is ineffective for an estimated 40% of epilepsy patients [1]. As an alternative to medication, surgical removal of the hippocampus (commonly, the origin of epileptic seizures) successfully cures epileptic seizures in about 70% of cases [2]; however, 50–90% of eligible patients forgo surgery due to risks associated with highly invasive brain surgery [2,3].

Magnetic resonance image-guided (MRI-guided) laser ablation of the hippocampus is a promising avenue for minimally invasive surgical treatment of epilepsy. Recent clinical trials using various needle-based, MRI-guided laser ablation systems to treat epilepsy have reported positive results; however, seizure outcomes were worse than those of epilepsy surgery [4]. These ablation systems exhibit one major limitation: linear needle trajectories are unable to traverse the entire curved structure of the hippocampus.

Steerable needles—comprising concentric tubes of pre-curved superelastic nitinol—address this limitation by enabling curvilinear needle trajectories in soft tissue. The potential benefits of curvilinear

trajectories are twofold: (1) they enable therapy delivery to a larger region of the hippocampus and (2) they enable accurate needle placement while avoiding sensitive, untreated tissue that might otherwise obstruct a typical linear trajectory [5]. To achieve curvilinear trajectories without shearing tissue, however, steerable needles must be deployed in a “follow-the-leader” (FTL) fashion, whereby the needle backbone follows the path created by the needle tip [5]. Precise coordination of needle insertion and rotation required for FTL deployment necessitates robotic actuation.

Research on MRI-compatible robotic needle-actuation systems has focused primarily on straight needle placement (see, e.g., Ref. [6]; for a more general review of MRI-compatible robotics, see Ref. [7]). To enable use of steerable needles for MRI-guided epilepsy surgery, we previously developed a compact, pneumatically actuated, additively manufactured, fail-safe, MR-compatible robotic needle-driving system [8]. This paper presents a joint-level trajectory coordinator for FTL deployment of a steerable needle using our MRI-compatible robot. FTL deployment is validated experimentally.

2 Methods

Our MRI-compatible robot system, shown in Fig. 1, uses a two degrees-of-freedom pneumatic stepper actuator to drive a helical steerable needle. The actuator is an additively manufactured monolithic structure comprising both a linear and a rotary flexible fluidic actuator (FFA). Actuation is achieved by inflation of the FFAs, causing translational or rotational deformation, respectively. Flat diaphragm grippers are inflated around clamshell inserts to grasp a transmission tube at the needle base. Detailed design, operation, and low-level nonlinear position control are presented in Ref. [8].

During operation, the superelastic needle deploys from a fixed, straight outer cannula (not shown in Fig. 1), and the distal end of the needle returns to its helical shape as it exits the cannula. Since a portion of the needle remains straightened inside the cannula, the displaced arc length and rotation of the deployed helix, respectively, equal the translation, x , and rotation, θ , of the needle base at the actuator. During FTL deployment, x and θ must be coordinated such that they follow the geometric relationship between helix arc length and rotation:

$$x = \theta \sqrt{r^2 + p^2} \quad (1)$$

where r and p are the helix radius and pitch, respectively.

To achieve FTL deployment using the stepper actuator, a joint-level trajectory coordinator determines the desired translation and rotation of the actuator (denoted by subscript des) during each actuation step. The trajectory coordinator accepts final desired displacements as inputs. For each actuation step (denoted by superscript k), the coordinator increases the desired rotation by a fixed step size, θ_{step} , which may be any fraction of the maximum rotational step size

$$\theta_{des}^k = \theta_{des}^{k-1} + \theta_{step} \quad (2)$$

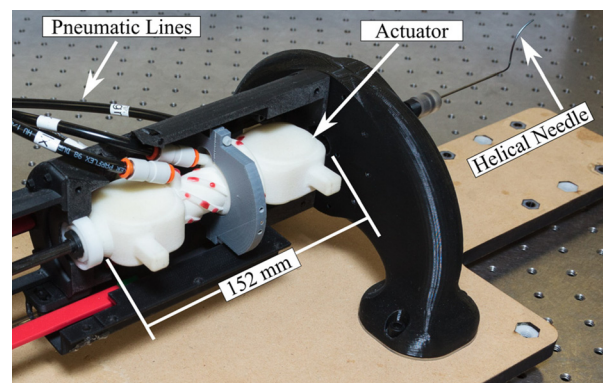


Fig. 1 Robot with helical steerable needle

¹Accepted and presented at The Design of Medical Devices Conference (DMD2016), April 11–14, 2016 Minneapolis, MN, USA.

DOI: 10.1115/1.4033242

Manuscript received March 1, 2016; final manuscript received March 17, 2016; published online May 12, 2016. Editor: William Durfee.

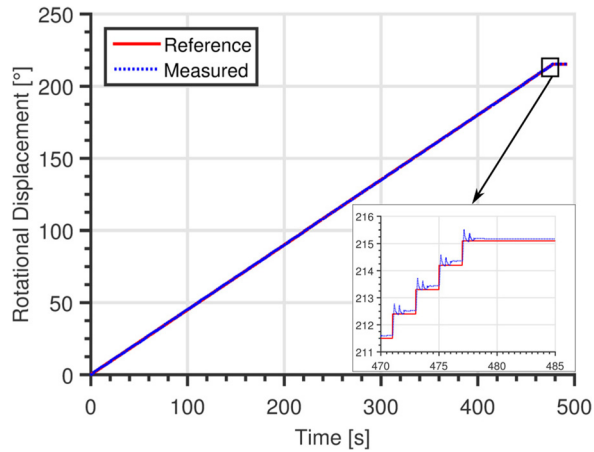


Fig. 2 Rotational displacement tracking

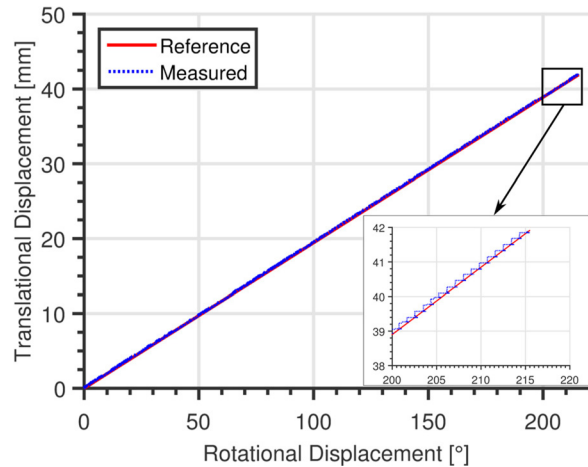


Fig. 4 FTL deployment

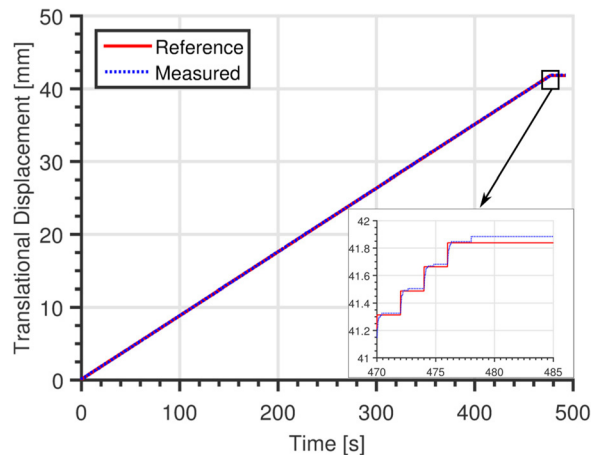


Fig. 3 Translational displacement tracking

and the desired translation is increased according to Eq. (1)

$$x_{\text{des}}^k = x_{\text{des}}^{k-1} + \theta_{\text{step}} \sqrt{r^2 + p^2} \quad (3)$$

until the desired displacements are saturated at their respective final values. The updated desired displacements are sent as inputs to the low-level position controller during each actuation step. The present actuator design is not capable of simultaneous translation and rotation, so each actuation step consists of a rotational substep followed by a translational substep. Beyond enforcing FTL conditions, this technique differs from previous implementations in that trajectory tracking by the low-level controller occurs during each step of the desired trajectory (not just in the vicinity of the final desired displacement).

To validate this trajectory coordinator for FTL needle deployment, a helical needle of radius 3.65 mm and pitch 10.53 mm/rad was deployed through a straight outer cannula into a gelatin-based phantom. Actuation substeps were performed at a frequency of 0.5 Hz (0.25 Hz full step frequency) and $\theta_{\text{step}} = 1$ deg. Needle position was measured using optical encoder hardware described in Ref. [8].

3 Results

Figures 2 and 3 show successful tracking of both the desired translational and rotational trajectories. The measured final translational error was 0.046 mm, and the measured final rotational displacement error was 0.072 deg. The small overshoot (at most 0.41 deg) seen in each rotary substep is negligible for the intended

application (see Ref. [8] for detailed performance specifications based on the intended clinical application). Furthermore, note that since the low-level position controller operates continuously during each actuation step, tracking errors do not accumulate from step-to-step, even as the desired displacement increases.

Figure 4 demonstrates the adherence to FTL conditions. The “reference” signal was calculated according to Eq. (1), using the measured angular displacement and helix geometric parameters. Small deviation from the FTL trajectory is observed at each substep due to the discrete rotational and translational substeps. The maximum deviation of the translational displacement from the FTL value was 0.25 mm, which is likely sufficiently small for the intended application. The final deviation of the translational displacement from the FTL value is zero within the resolution of encoder hardware.

4 Interpretation

This technical brief presented a joint-level trajectory coordination technique for FTL deployment of a helical steerable needle using a previously developed MRI-compatible robotic system with stepper actuators. Experimental results using the proposed trajectory coordinator demonstrated FTL needle deployment that is sufficiently accurate for the intended clinical application of needle-based surgical treatment of epilepsy. Future work will include ex vivo targeting experiments with MRI guidance.

References

- [1] Kwan, P., and Brodie, M. J., 2000, “Early Identification of Refractory Epilepsy,” *N. Engl. J. Med.*, **342**(5), pp. 314–319.
- [2] Lhatoo, S. D., Solomon, J. K., McEvoy, A. W., Kitchen, N. D., Shorvon, S. D., and Sander, J. W., 2003, “A Prospective Study of the Requirement for and the Provision of Epilepsy Surgery in the United Kingdom,” *Epilepsia*, **44**(5), pp. 673–676.
- [3] de Flon, P., Kumlien, E., Reuterwall, C., and Mattsson, P., 2010, “Empirical Evidence of Underutilization of Referrals for Epilepsy Surgery Evaluation,” *Eur. J. Neurol.*, **17**(4), pp. 619–625.
- [4] Willie, J. T., Laxpati, N. G., Drane, D. L., Gowda, A., Appin, C., Hao, C., Brat, D. J., Helmers, S. L., Saindane, A., Nour, S. G., and Gross, R. E., 2014, “Real-Time Magnetic Resonance-Guided Stereotactic Laser Amygdalohippocampotomy for Mesial Temporal Lobe Epilepsy,” *Neurosurgery*, **14**(6), pp. 569–585.
- [5] Gilbert, H. B., Neimat, J., and Webster, R. J., 2015, “Concentric Tube Robots as Steerable Needles: Achieving Follow-the-Leader Deployment,” *IEEE Trans. Rob.*, **31**(2), pp. 246–258.
- [6] Li, G., Su, H., Cole, G., Shang, W., Harrington, K., Camilo, A., and Fischer, G. S., 2015, “Robotic System for MRI-Guided Stereotactic Neurosurgery,” *IEEE Trans. Biomed. Eng.*, **62**(4), pp. 1077–1088.
- [7] Fisher, T., Hamed, A., Vartholomeos, P., Masamune, K., Tang, G., Ren, H., and Zion, T. H., 2014, “Intraoperative Magnetic Resonance Imaging—Conditional Robotic Devices for Therapy and Diagnosis,” *Proc. Inst. Mech. Eng., Part H*, **228**(3), pp. 303–318.
- [8] Comber, D. B., Slightam, J. E., Gervasi, V. R., Neimat, J. S., and Barth, E. J., 2016, “Design, Additive Manufacture, and Control of a Pneumatic, MR-Compatible Needle Driver,” *IEEE Trans. Rob.*, **32**(1), pp. 138–149.